Stress and Fracture Analyses of Nuclear Power Plant LP Turbine Rotor Discs

Choon-Yeol Lee*, Jae-Do Kwon, Young S. Chai
Department of Mechanical Engineering, Yeungnam University
Ki-Sang Jang
Korea Electric Power Research Institute

Fracture phenomenon has been reported on blades, rotors, connections and rotor discs of LP turbines of nuclear power plants, which is caused by fatigue, stress corrosion and erosion. In this study, as a tool of reliability evaluation, a number of stress and fracture analyses were performed on the defected area under various operating conditions using the finite element method. Possible defects on key-way and rotor disc were assumed to be two-dimensional cracks and centrifugal force, temperature distribution and shrink-fit effect were included as external loads. From stress analysis results, stress intensity factors were obtained and these values can be utilized to evaluate reliability and predict remaining lifetime of the turbine discs.

Key Words : Nuclear Power Plant, LP Turbine, Fracture Analysis, Finite Element Method, Reliability Evaluation, Remaining Lifetime

1. Introduction

As commercial running time of domestic nuclear power plants is getting longer, there is more possibility to find defects and cracks around key-way and rim of turbine rotor discs at periodical evaluation, which causes more frequent operation stops. Hence, it is getting more important to evaluate reliability (Lee, Kim and Ha, 1995; Nahm, Kim and Yu, 1998) and to predict remaining lifetime of the nuclear power plants (Jeon, 1987; Kim et al., 1999).

According to the survey for the causes of operation stops in domestic nuclear power plants between 1985 and 1988, fifty cases were caused by defects in the system of turbine and generator out of 128 cases in total. Especially in turbine, it has been reported that the defects are mainly caused by fatigue, stress corrosion and erosion in blades, connections of blade and disc and rotor discs.

In this study, stress analyses on LP turbine rotor discs were carried out for A and B nuclear power plants. The stress analysis results are used to calculate stress intensity factors, SIF, for possible cracks with arbitrary sizes at arbitrary locations. Once the sizes and locations of cracks are found by nondestructive inspection (Chang et al., 1997), these resultant stress intensity factors will be applied and therefore reliability evaluation, inspection period determination and remaining lifetime prediction will be performed. For this purpose, a GUI (Graphical User Interface) computer program was also developed based on the experimental and computational results to help plant operators to apply them to each turbine rotor disc conveniently.

2. Nuclear Power Plant Turbine

In domestic nuclear power plants, tandem compound type turbines were commonly adopted, where each axis of turbine is directly connected to a generator as shown in Fig. 1. And in a number

* Corresponding Author,
E-mail : cylee@ynucc. yu. ac. kr
TEL : +82-53-810-2570 ; **FAX** : +82-53-813-3703
Department of Mechanical Engineering, Yeungnam University, 214-1 Daedong, Kyungsansi, Kyungbuk, 712-749 Korea. (Manuscript **Received** June 5, 1999; **Revised** October 30, 1999)

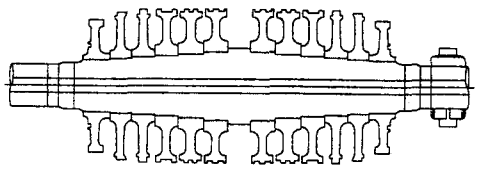

Fig. 1 Configuration of power plant LP turbine (Plant B)

of domestic major nuclear power plants, including the nuclear power plant A and B, shrunk-on type turbine rotor discs were utilized.

A shrunk-on type rotor disc is composed of key-way, disc hub, rim and locking-pin which prevents disc on axis from sliding and blades are attached to a disc rim as shown in Fig. 2. This shrunk-on type rotor disc is designed to overcome centrifugal force and subject to general dynamic loads including temperature distribution, vibration, thrust and so on. LP turbine rotor discs are usually made of 3.5% NiCrMoV alloy which is strong against erosive environment.

3. Loads in Turbine Rotor Disc

A shrunk-on type turbine rotor disc is assembled to an axis by shrink-fitting so that contact and friction force developed between rotor disc and axis transmit rotational force. Generally, the amount of shrink-fitting is designed in such a way that the contact force is equal to centrifugal force due to rotation when rotational speed reaches 130% of operating speed, so called lift-off speed. This contact force results in hoop stress of the rotor disc and compressive stress of the axis in circumferential direction. Moreover, rotor disc is subject to centrifugal force and temperature distribution loads at operation starts and stops. These external loads cause and develop defects and cracks at the corners of rim and rotor disc, where stress concentration occurs. Possible locations of frequent defects and cracks are illustrated in Fig. 2.

In this paper, a number of finite element analyses were performed on the shrunk-on type rotor disc considering contact and centrifugal force and temperature distribution.

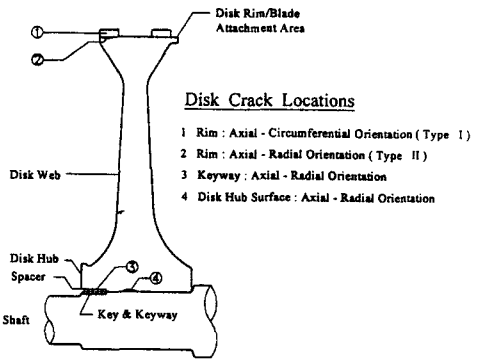

Fig. 2 Locations of cracks on the LP rotor disc

4. Fracture Analysis Using Finite Element Method

Inevitably, defects or cracks happen during manufacturing process and operation. Stress intensity factor, K, is generally used as a representing fracture parameter determining safety and remaining lifetime and has been obtained by many researchers for cracks with various geometry under general loads. As mentioned previously, frequently defected areas are key-way, rim and disc hub, where generally three dimensional cracks are found.

In this study, since fracture analyses should be performed for many possible locations and crack sizes, only two dimensional penetration cracks in axial direction were considered to avoid complex and time consuming three dimensional analysis. This assumption is based on the following facts. First, cracks in axial direction is more apt to grow than those in circumferential direction. Secondly, the analysis results from two dimensional penetration crack are more conservative than those from three dimensional crack.

In order to perform two dimensional finite element analyses, the method of superposition was used with two 2-dimensional models, which are shown in Figs. 3, 4 and 9. As shown in Figs. 3 and 9, the two dimensional axisymmetric models are composed of an axis and discs with $y-z$ symmetric plane. With this model, two dimensional axisymmetric analysis was performed and centrifugal force, shrink-fitting effect and temperature distribution were considered in ap-

Table 1 Material properties of the turbine rotor disc (Plant A and B)

Young's modulus, E (Pa)	2.06×10^{11}
Poisson's ratio, ν	0.3
Coeff. of thermal expansion, a(1/℃)	12.00×10^{-6}
Thermal conductivity, χ(W/m K)	54.0
Density, ρ(kg/m^3)	7.833×10^3

Table 2 Temperature distribution of the turbine rotor disc of Plant A

Disc No.	Stage No.	Outer temperature(℃)
1	1	216
	2	162
2	3	128
	4	110
3	5	93
4	6	77
5	7	55
6	8	36

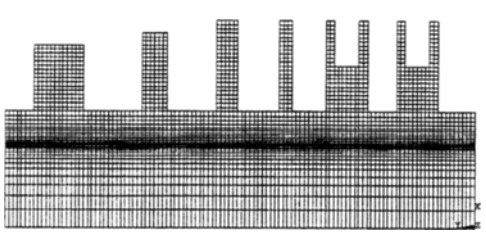

Fig. 3 Axisymmetric modelling of the rotor disc of Plant A

plying boundary conditions.

4.1 Stress analyses on Plant A

The LP turbine of nuclear power Plant A consists of six discs and the first two discs have two sets of and blades. Material properties and the axisymmetric model used for these analyses are shown in Table 1 and Fig. 3, respectively. In the axisymmetric model, 4983 nodes and 4669 rectangular elements were used. At the contact surface of shaft, node to node contact elements were used to simulate shrink-fitting effect. The

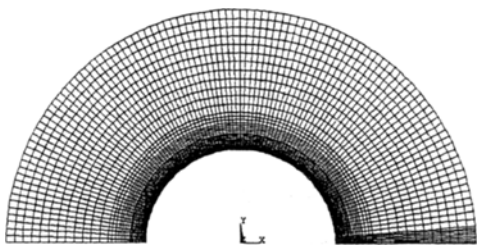

Fig. 4 Finite element model of a crack on a disc (Plant B)

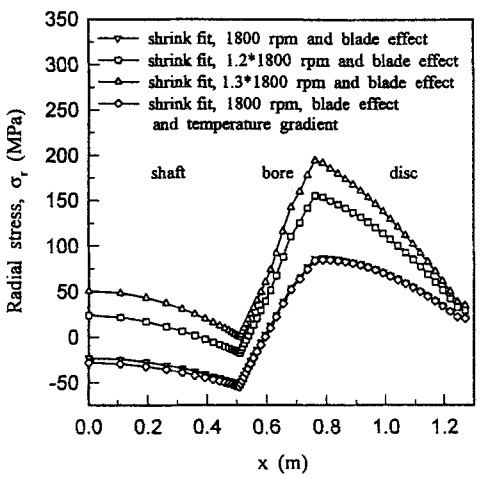

Fig. 5 Radial stress distribution of the fifth disc (Plant A)

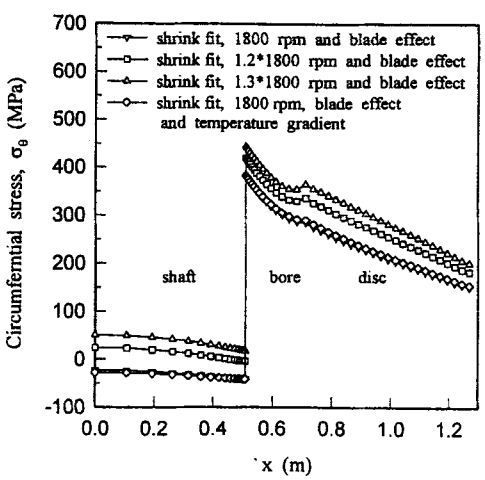

Fig. 6 Circumferential stress distribution of the fifth disc (Plant A)

amount of shrink-fitting was set 0.2% as designed. Also, temperature distribution at normal operating condition, which is shown in Table 2, was

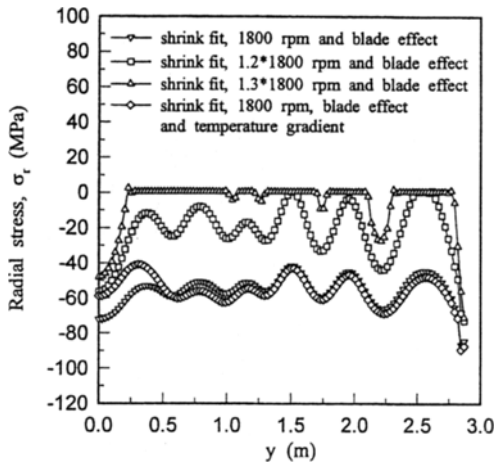

Fig. 7 Radial stress distribution along shaft at the interface of shaft and disk hub (Plant A)

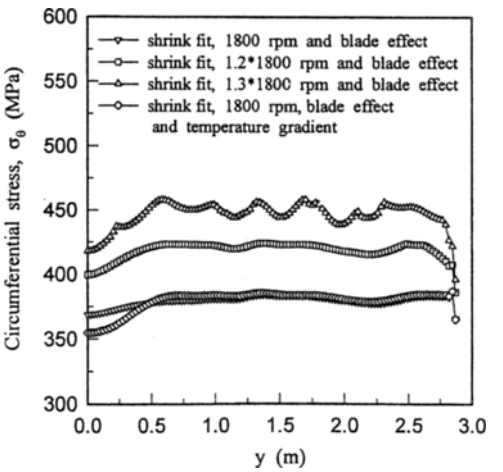

Fig. 8 Circumferential stress distribution along shaft at the interface of shaft and disc hub (Plant A)

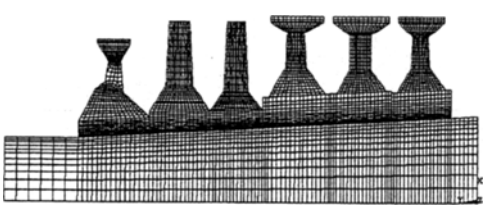

Fig. 9 Axisymmetric modelling of the rotor disc of Plant B

applied to each stage. Centrifugal force was obtained considering mass of blades and rotating speed and applied to the end of disc where blades are attached.

In Figs. 5 and 6, illustrated are calculated radial and circumferential stresses at the fifth disc due to these external loads along radial direction, among which the circumferential stress will be utilized as crack opening load. It should be noted that the circumferential stress has a discontinuity on the shaft surface because of contact force caused by shrink-fitting and that the radial stress has discontinuity in slopes due to variance in thickness of shaft, disc hub and disc. These resultant stress distributions were applied to a plane strain model shown in Fig. 4 which involves a penetration crack with crack size, a and subsequently a fracture analysis was performed to calculate the stress intensity factor K_I. This procedure was repeated according to various crack locations and sizes and the displacement extrapolation method was used at the crack tip for K_I calculation.

In Figs. 7 and 8, resulting radial(contact) and circumferential stress distributions along the axis are illustrated. It shows that the circumferential stress increases and the radial stress decreases as the rotating speed increases. From these figures, it can also be seen that the radial stress vanishes almost everywhere except the fifth and sixth stages when rotating speed reaches 130% of operating speed. Also, the centrifugal force was turned out to be the most effective loading and temperature distribution was not effective on resulting radial stress.

4.2 Stress analyses on Plant B

The LP turbine of nuclear power Plant B consists of six discs and the first disc has three sets of blades, the second and third discs have two sets of blades each and the forth, fifth and sixth discs have a set of blades, respectively.

The analysis procedure was similar to that of Plant A, and the axisymmetric model and the temperature distribution used for the analysis are shown in Fig. 9 and Table 3, respectively. In the axisymmetric model, 5254 nodes and 4955 rectangular elements were used and the rest of analysis is similar to that of Plant A.

In Figs. 10 and 11, resulting radial and circum-

Table 3 Temperature distribution of the turbine rotor disc of Plant B

Disc No.	Outer temperature(℃)
1	260.00
2	223.84
3	187.66
4	151.49
5	115.32
6	79.15

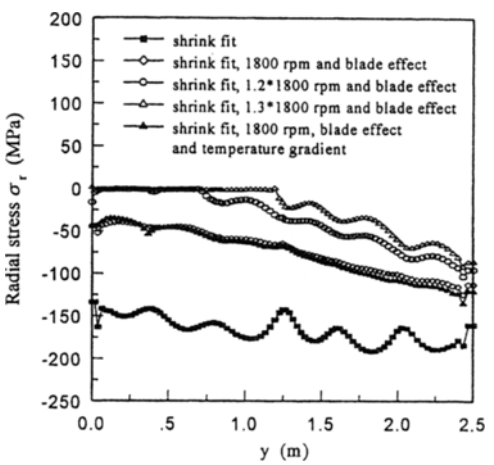

Fig. 10 Radial stress distribution along shaft at the interface of shaft and disc hub (Plant B)

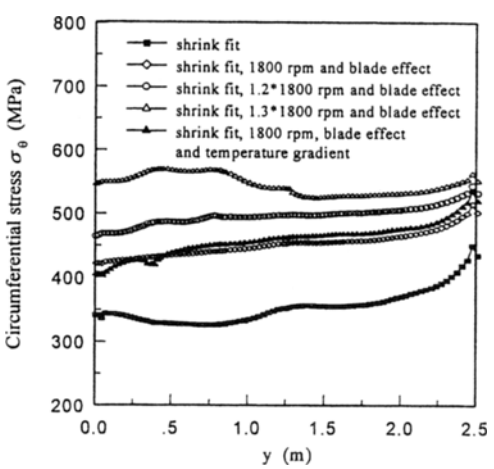

Fig. 11 Circumferential stress distribution along shaft at the interface of shaft and disc hub (Plant B)

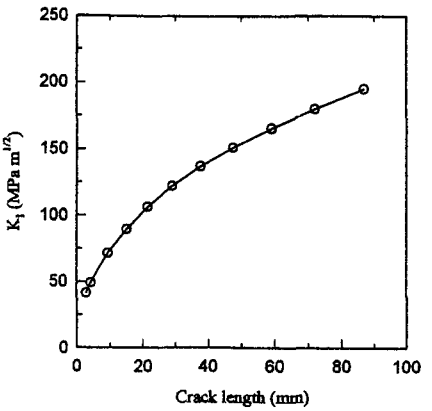

Fig. 12 The variation of stress intensity factor along crack length at disc no. 4(Plant A)

ferential stress distributions along the axis are illustrated. It shows that the circumferential stress increases and the radial stress decreases as the rotating speed increases as observed from Plant A analyses. Also, the temperature distribution does not have much contribution on resulting radial stress.

4.3 Fracture analysis

Fracture analyses were performed on the turbine rotor discs of Plant A and B based on the stress analysis results with contact and centrifugal force and temperature distribution at normal operating speed(1800rpm). In these analyses, degenerated singular 8-node elements are used at the crack tip and regular 8-node elements were used elsewhere as shown in Fig. 4. Stress intensity factors were obtained for various cracks with ranging from 0.3mm to 100mm depending on the diameter of each stage and disc.

In order to utilize resulting stress intensity factors in calculating remaining lifetime, a least square curve fitting was applied to relate crack length with stress intensity factors.

Fig. 12 shows the relation between crack length and the stress intensity factor obtained from the forth rotor disc with radial cracks. In Fig. 13, the stress intensity factors obtained at the surface between fifth and sixth discs(hub no. 6) are illustrated. Since the normalized crack size, a/W, is much smaller than that of disc hub surface without disc, the stress intensity factor shows

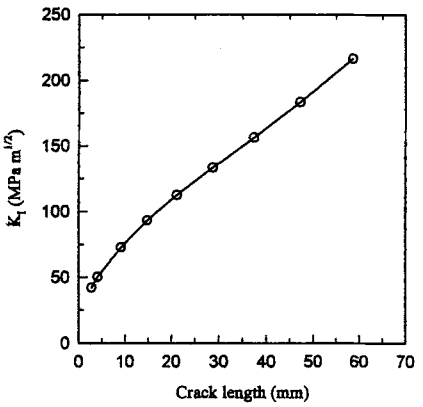

Fig. 13 Stress intensity factor along crack length at hub no. 6 (Plant A)

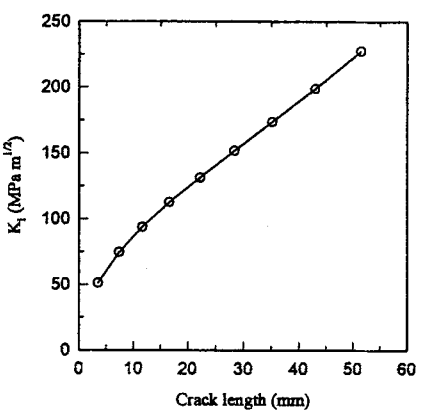

Fig. 14 The variation of stress intensity factor along crack length at disc no. 2 (Plant B)

asymptotic behavior of $a^{1/2}$. On the other hand, at the disc hub surface without disc, the stress intensity factor does not show such asymptotic behavior because of smaller uncracked ligament and relatively larger crack size.

A similar fracture analysis was performed on turbine rotor discs of Plant B. Stress intensity factors were obtained for various crack sizes at both inlet and outlet of each stage. In Figs. 14 and 15, illustrated are resulting stress intensity factors, which do not show asymptotic behavior since crack size is relatively large.

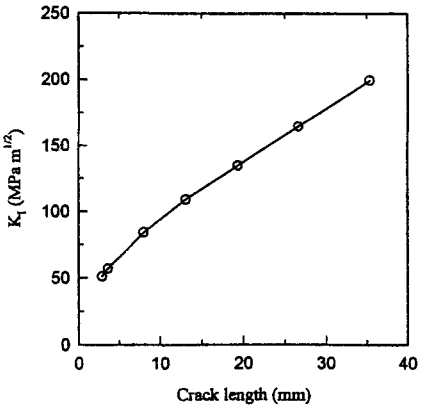

Fig. 15 The variation of stress intensity factor along crack length at disc no. 5 (Plant B)

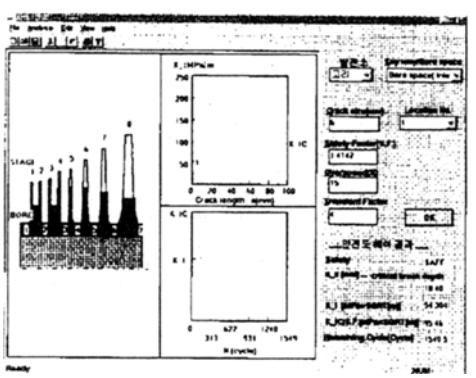

Fig. 16 GUI data input display of SAFE (Plant A)

5. Development of a Computer Program for Reliability and Remaining Lifetime

Based on resulting stress intensity factors, a computer program, SAFE, was developed to evaluate reliability and to predict remaining lifetime of turbine discs. For the convenience of users, this program was developed based on GUI environment as shown in Fig. 16.

5.1 Reliability

There are many codes concerning brittle fracture such as ASME Sec. X1 (Boiler and Pressure Vessel Code), BSI PD 6493 of Standard Institution and WES 2805. This computer program evaluate reliability according to ASME Sec. XI.

Fracture toughness, K_{IC}, for the material mentioned above was obtained by experiments,

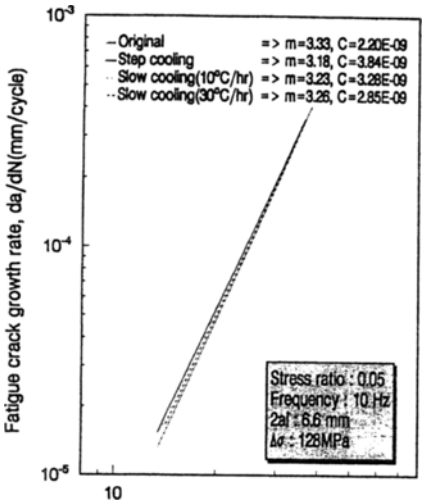

Fig. 17 Straight lines by the least square method for original, step cooled, slow cooled (10℃/hr) and slow cooled (30℃/hr) materials

details of which is not included in this paper. In general, K_{IC} depends on temperature, but in this study the smallest value of 135 MPa$\sqrt{m}$ at room temperature is used to avoid a large number of experiments and to keep results conservative.

5.2 Remaining lifetime

The following describes Paris' law, which is commonly used to calculate remaining lifetime

$$\frac{da}{dN}=C(\Delta K)^m$$

where C and m are found to be 2.20×10^{-9} and 3.33 by experiments, the results of which are shown in Fig. 17 (KEPRI, 1996). The program SAFE calculates remaining lifetime by integration of this Paris' law with ΔK obtained transient stress analysis during transient state, which is not included in this paper (EPRI, 1988).

6. Conclusions

In this study, stress and fracture analyses are performed on defects or cracks occurring at turbine rotor discs and the following conclusions are achieved.

(1) Based on stress analysis result, centrifugal force is found to be most effective during steady state and 130% of overspeed compensates shrink-fitting in both of A and B plants.

(2) From fracture analysis, as expected, stress intensity factor shows asymptotic behavior of $a^{1/2}$ where crack size is relatively small. And it is found that disc hub surface, where radius and centrifugal force are small, has smaller stress intensity factor than key-way.

(3) A computer program is developed, which contains these computational results combined with experimental properties. This program is convenient and useful in evaluating reliability and predicting remaining lifetime of the turbine discs with given crack size and location by non-destructive inspection and transient state stresses.

References

Broek, D., 1986, *Elementary Engineering Fracture Mechanics*, Martinus Nijhoff Publishers.

Chang, H. K., Cho, K. S., Won, S. H., Chung, M. H., Cho, Y. S. and Hur, K. B., 1997, "Development of an Ultrasonic Inspection Technique for LP Turbine Rotor Disc," *KSME*, Vol. 17, No. 3, pp. 174~183. (in Korea)

EPRI, 1988, "Improvements to the SAFER Code Rotor Lifetime Prediction Software," *Life Assessment Methodology for Turbogenerator Rotors*, Vol. 1, EPRI CS/EL-5593, Projects 2481-3, 2785-1 Final Report.

EPRI, 1988, "SAFER Code Methodology Tutorial for Turbine Rotor Lifetime Estimation," *Life Assessment Methodology for Turbogenerator Rotors*, Vol. 3, EPRI CS/EL-5593, Projects 2481-3, 2785-1 Final Report.

EPRI, 1988, *Nondestructive Evaluation of Turbines and Generator*, EPRI Report, EPRI WS-80-133.

Hohn, A., 1973, *Rotors for Large Steam Turbine*, Brown Boveri Rev., Vol. 9, pp. 404~416.

Jeon, J. Y., 1987, "The Life Estimation of Turbine Rotor through Fracture Mechanics and Fatigue Analysis(Ⅰ)," *KSME*, Vol. 11, No. 4, pp. 537~548. (in Korea)

KEPRI, 1996, *Development of the Ultrasonic*

Inspection Technique for Turbine Rotor Disc and Boreless Shaft (Evaluation of Integrity for Turbine Rotor Disc), KEPRI-93G-J04.

Kim, H. S., Kim, Y. J., Suh, M. W. and Hong, K. T., 1999, "Development of Life Prediction Program for High Pressure Turbine Rotor for Power Generation," *KSME*, Vol. 23, No. 3, pp. 434~441. (in Korea)

Lee, K. Y., Kim, J. S. and Ha, J. S., 1995, "Determination of Stress Intensity Factors for Embedded Elliptical Crack in Turbine Rotor," *KSME*, Vol. 19, No. 5, pp. 1229~1242. (in Korea)

Murakami, Y. 1987, *Stress Intensity Factors Handbook*, Vol. 1 & 2, The Society of Material Science, Pergamon Press.

Nahm, S. H., Kim, A. and Yu, K. M., 1998, "Nondestructive Evaluation of Toughness Degradation of 1Cr-1Mo-0. 25V Steel Using Electrical Resistivity," *KSME*, Vol. 22, No. 5, pp. 814~820. (in Korea)

Owen, D. R. J. and Griffiths, J. R., 1973, "Stress Intensity Factors for Cracks in a Plate Containing a Hole and in a Spinning Disc," International Journal of Fracture, Vol. 9, pp. 471~476.

Rolfe, S. T., and Barsom, J. M., 1977, *Fracture and Fatigue control in Structures*, Prentice-Hall, pp. 140~166.

Swanson Analysis Systems, Inc., 1992, *ANSYS User's Manual for Revision 5.0*, Vol. Ⅳ Theory.

Tada, H., Paris, P. C. and Irwin, G. R., 1985, *The Stress Analysis of Cracks Handbook*, Paris Production Inc. and Del Research Corporation.